Virial expansion coefficients in the harmonic approximation

J. R. Armstrong, N. T. Zinner, D. V. Fedorov, and A. S. Jensen
Department of Physics and Astronomy, Aarhus University, DK-8000 Aarhus C, Denmark
(Received 11 May 2012; revised manuscript received 29 June 2012; published 15 August 2012)

The virial expansion method is applied within a harmonic approximation to an interacting N-body system of identical fermions. We compute the canonical partition functions for two and three particles to get the two lowest orders in the expansion. The energy spectrum is carefully interpolated to reproduce ground-state properties at low temperature and the noninteracting high-temperature limit of constant virial coefficients. This resembles the smearing of shell effects in finite systems with increasing temperature. Numerical results are discussed for the second and third virial coefficients as functions of dimension, temperature, interaction, and transition temperature between low- and high-energy limits.

DOI: 10.1103/PhysRevE.86.021115 PACS number(s): 05.30.−d, 05.70.−a, 67.10.Fj, 21.10.Ma

I. INTRODUCTION

The virial expansion is a classical concept [1–4] that has been extended to be applicable for quantum mechanical systems [5]. The expansion is in terms of few-body correlations and therefore is most efficient when the influence of N-body effects decreases with N. In practice, this decrease has to be very fast because higher-order correlations are extremely difficult to obtain by accurate calculations. This fact is not obvious since only the spectrum of N interacting particles is needed, not wave functions or structures nor any other properties. However, obtaining these spectra implies solving the N-body problem, which is already demanding beyond two particles for general interactions.

In the classical textbook by Huang on statistical mechanics [6], the virial expansion is discussed for the quantum mechanical case and it is elegantly demonstrated how the second virial coefficient can be obtained from knowledge of the two-body scattering phase shift and bound-state spectrum (when present). This was subsequently generalized in the seminal paper of Dashen, Ma, and Bernstein [7] where a formulation of statistical mechanics in terms of the scattering S matrix is given. The formulation gives a prescription for calculating virial coefficients at any order, and shortly thereafter the behavior of the third-order coefficient at low temperature was obtained via the S-matrix method [8]. The S-matrix approach to virial coefficients is still an active research topic [9] with recent applications in the field of cold atomic gases [10]. However, since determining the S matrix in a general system with multiple particles is a highly nontrivial task, it is valuable to pursue alternative ways of approaching the virial expansion.

Approximations or assumptions are unavoidable at some point. The traditional strategies have been either to limit the Hilbert space allowed for the variational many-body wave functions or to design schematic Hamiltonians aiming for specific features. The latter approach requires great care and physical intuition to retain the necessary features of the Hamiltonian that will accurately describe the phenomena under study. An approach along this second line of reasoning is the use of harmonic Hamiltonians where interaction terms are replaced by harmonic oscillators. This is extremely convenient from a computational point of view as many aspects become analytically addressable for both fermionic and bosonic systems [11–14].

The replacement of one- and two-body terms in the Hamiltonian by harmonic forms leaves the problem of determining the parameters of the harmonic Hamiltonian according to given criteria. Here one must again take guidance from physical properties and aspects of the system that are crucial for the system under study. Recently, we formulated an approach that explores the N-body problem in an external parabolic confining potential by fixing the two-body interactions to the properties of an exactly solvable problem in the same geometry [15]. The two-body information needed is the energy eigenvalues and structural properties of the wave function such as radial averages.

The example studied in Ref. [15] was short-range interacting particles in a harmonic trap for which the two-body problem can be exactly solved in the zero-range limit [16]. Within the field of cold atomic gases, this solution was subsequently confirmed by different experimental groups [17]. The model studied in Ref. [16] has since been used as a starting point in both nuclear and cold atomic gas physics [18]. Recently, the harmonic approximation with parameters fixed to exact two-body properties has been applied to particles that interact via dipole forces [19–23] and shown to accurately reproduce numerical few-body results for moderate to strong dipole strengths [24–27].

This harmonic method has also been extended to the thermodynamical regime at finite temperature [11,12,28], where it has been shown using a path-integral formalism that the canonical partition function for a given particle number can be obtained [11,14,29–31]. Here we consider an alternative approach that uses exact diagonalization of the Hamiltonian and subsequent calculation of the relevant degeneracies in the energy spectrum for a given number of particles [28]. This is in contrast to the usual approximation using the grand partition function where only the average particle number is conserved. The method applies to both identical bosons and fermions as well as distinguishable particles and combinations of all these possibilities [15,20,28]. The difficult part is to find the degeneracies of the N-body spectrum for the specified symmetries required by quantum statistics. The energies themselves are easily found from the harmonic oscillator solutions.

Here we consider the virial expansion within the harmonic Hamiltonian approximation for identical fermions. This paper

is a natural extension of Ref. [28], where the thermodynamics of small to moderate size systems of fermions and bosons was considered by direct computation of the partition function. This requires a numerically efficient determination of the level degeneracies, which, however, is possible only up to moderate particle numbers ($N \sim 20$) even in a harmonic model. The virial expansion is usually a rapidly converging series and we therefore expect to be able to compute coefficients within the harmonic approach. However, there are some subtleties with the convergence of the coefficients that must be carefully handled. Therefore we focus almost exclusively on the formal development of the virial expansion within the harmonic approximation.

A motivation for our work is the recent investigation of universal thermodynamics within cold atomic gas experiments [32] where the virial expansion has been successfully applied [33]. However, the expansion is general and is applicable to other fermionic systems. While the typical condensed-matter and cold atom fermion systems have two internal (spin or hyperfine spin) components, we consider the case of single-component fermions here in order to keep the formalism simple while still retaining the full quantum statistical properties of a Fermi system. Multicomponent fermionic and bosonic systems will not be considered in this study.

The purpose of the present paper is to formulate and explore the harmonic method and the virial expansion to prepare for future applications to systems in both cold atomic gases and nuclear physics as well as condensed-matter systems. The paper is organized as follows. We describe the ingredients of the method in Sec. II. Numerical illustrations for the lowest virial coefficients follow in Sec. III. In Sec. IV we summarize and provide an outlook for future directions of interest.

II. THEORY

We first present general definitions of the crucial ingredients. Then we apply the formulation to the results of a system of N particles described by a coupled set of harmonic oscillator potentials. The approach to the high-temperature limit is finally modified to exhibit the behavior corresponding to the correct high-energy spectrum.

A. Basic definitions

The classical virial expansion is an expansion of the equation of state of a gas of identical particles, usually in powers of the number density ρ (see, e.g., Refs. [1–4]):

$$p = k_B T \rho [1 + B_2(T)\rho + B_3(T)\rho^2 + \cdots], \tag{1}$$

where p is the pressure, k_B is Boltzmann's constant, T is the temperature, and the B_i's are the virial coefficients of the expansion. In the classical expansion, they are related to the intermolecular or interatomic potentials of i interacting particles. The advantage of the expansion is that it reveals deviations from ideal gas behavior by examining just the few-body aspects of the system. The leading term is then the ordinary ideal gas expression for a non-interacting system. The second term in the classical expansion in three dimensions is given by the B_2 coefficient

$$B_2 = -\frac{1}{2}\int \{\exp[-\beta V_{12}(r)] - 1\} d^3 r, \tag{2}$$

where V_{12} is the interparticle potential depending on the relative coordinate r and $\beta = 1/k_B T$. The integral in Eq. (2) is known as a configuration integral and from it one can see that this coefficient converges only for potentials that decay faster than $1/r^3$. The convergence in two dimensions is correspondingly achieved only when V decays faster than $1/r^2$. The general coefficient is

$$B_i = -\frac{i-1}{i!V}\sum \mathcal{I},$$

where V is the volume of the system and $\mathcal{I}$ denotes all independent i-cluster integrals. The i-cluster integrals are all the independent clusters containing the i particles, first presented graphically in Ref. [34]. A cluster in this context can be visualized graphically by thinking of i numbered circles with lines connecting them symbolizing the interaction between those particles. These lines can be drawn in many different ways; the only requirement for the i cluster is that all i atoms or molecules must be connected to at least one other member of the system. The quantum mechanical version of the cluster expansion was developed at around the same time in Ref. [5].

For a system of quantum mechanical particles with Fermi or Bose statistics, the expansion is most commonly performed in the fugacity $z = \exp(\beta\mu)$ of the system, where μ is the chemical potential of the N-body system. The grand canonical partition function $\mathcal{Z}$ is written as an expansion in z,

$$\mathcal{Z} = 1 + zQ_1 + z^2 Q_2 + \cdots, \tag{3}$$

which translates into an expansion for the grand thermodynamic potential Ω,

$$\Omega = -k_B T Q_1 [z + b_2 z^2 + b_3 z^3 + \cdots]. \tag{4}$$

The first virial coefficients can be explicitly written

$$b_2 = \left(Q_2 - Q_1^2\right)/Q_1, \tag{5}$$

$$b_3 = \left(Q_3 - Q_1 Q_2 + Q_1^3/3\right)/Q_1, \tag{6}$$

$$b_4 = \left(Q_4 - Q_1 Q_3 + Q_1^2 Q_2 - Q_2^2/2 - Q_1^4/4\right)/Q_1, \tag{7}$$

where Q_N is the canonical partition function for N particles of the proper symmetry, that is,

$$Q_N = \sum_j g_j^{(N)} \exp\left(-\beta E_j^{(N)}\right), \tag{8}$$

where $g_j^{(N)}$ and $E_j^{(N)}$ are the degeneracy and energy of the jth state of the N-body system. Thus Q_N can be calculated solely from the energy spectrum of the N-body system and all thermodynamic quantities can then be obtained from Ω in Eq. (4) to the order desired. The classical virial expansion [Eq. (1)] can be recovered from the quantum version introduced above by using $\langle N\rangle = -\frac{\partial\Omega}{\partial\mu}|_{T,V}$ and $\Omega = -pV$ (see, for instance, Ref. [35], where the relation of B_i and b_i is also discussed). In the present case we have an external trap and the volume must be suitable translated into parameters of the trap before making detailed comparisons to experiments or other studies [36].

In practical calculations, it is more convenient to consider the difference between interacting and noninteracting systems. We then consider the differences $\Delta Q_n = Q_n - Q_n^{(1)}$ and $\Delta b_n = b_n - b_n^{(1)}$, where the superscript (1) denotes a noninteracting system having the same N-body fugacity z. We can then rewrite Eq. (4) as

$$\Omega = \Omega^{(1)} - k_B T Q_1[\Delta b_2 z^2 + \Delta b_3 z^3 + \cdots], \tag{9}$$

where $\Omega^{(1)}$ is the grand thermodynamic potential of the noninteracting system with the same fugacity. The differences of the virial coefficients in Eqs. (5)–(7) become

$$\Delta b_2 = \Delta Q_2/Q_1, \tag{10}$$

$$\Delta b_3 = \Delta Q_3/Q_1 - \Delta Q_2, \tag{11}$$

$$\Delta b_4 = \Delta Q_4/Q_1 - \Delta Q_3 + Q_1 \Delta Q_2 - \left((Q_2)^2/2 - \left(Q_2^{(1)}\right)^2/2\right)/Q_1. \tag{12}$$

These definitions and expressions are general and now applicable to a specified set of potentials producing the partition functions Q_n and the corresponding (differences of) virial coefficients.

B. Harmonic approximation

The one- and two-body interactions for the N-body system are approximated by second-order polynomials in Cartesian coordinates. The Hamiltonian is a sum of similar terms from each spatial dimension $H = H_x + H_y + H_z$. In the present work we consider the two- and three-dimensional cases. For identical particles of mass m the Hamiltonian of the x direction is

$$H_x = -\frac{\hbar^2}{2m}\sum_{k=1}^{N}\frac{\partial^2}{\partial x_k^2} + e\frac{1}{8}m\omega_{\rm in}^2\sum_{i,k=1}^{N}(x_i - x_k)^2 + \frac{1}{2}m\omega_0^2\sum_{k=1}^{N}x_k^2 + \frac{N(N-1)}{2}V_{sx}, \tag{13}$$

where x_i is the coordinate of particle i, ω_0 and $\omega_{\rm in}$ are frequencies of the one- and two-body interactions, and V_{sx} is a constant adjusting the energy to the desired value. The factor 1/8 in the second term comes from the use of the reduced mass equal to $m/2$ and to avoid double counting in the sum.

The frequencies and the constant shift can be chosen to reproduce certain properties of a modeled system as discussed in Ref. [15]. How these parameters are chosen does not affect the computation of the virial coefficients, which therefore are obtained as functions of the parameters in the Hamiltonian. The method is general and applicable as soon as a Hamiltonian of the oscillator form is available. It is, however, still useful to illustrate by describing the procedure for a specific system. We focus on a system of identical, spin-polarized fermions confined in an external trap [15] where the fermions interact via a short-range potential. Due to the Pauli principle, the particles cannot interact in the spherical s-wave channel and the lowest nontrivial interaction will be odd and of the p-wave kind (higher odd partial wave channels will be neglected). In the zero-range limit, the model of Busch *et al.* [16] can still be solved for p-wave interactions in both three- [37] and two-dimensional [38] traps. We adjust the interacting frequency $\omega_{\rm in}$ to reproduce some property related to the spatial extension of the correct two-body wave function (the average square radius in the two-body ground state in the trap). The shift V_{sx} is then added to make sure that the exact two-body ground-state energy is reproduced by the oscillator potential. Notice that this (constant) energy shift does not influence thermodynamics in any essential way. We therefore ignore it for most of our discussion, except for some comments near the end of Sec. III.

The accuracy of the harmonic approximation should depend on the degree to which the physical two-body potential allows a quadratic expansion. Naively, this should be the case for potentials that have a sizable attractive pocket, which is true for many molecular potentials that allow a large number of bound states [39]. An example is the Morse potential, which has been explored in the harmonic approximation in Ref. [14]. As mentioned in the Introduction, for dipolar particles, the harmonic approximation is extremely accurate, even in the regime of small dipole moments when suitable adjustment of the harmonic frequency is performed [19–21]. In fact, even when the real potential is shallow, the energy can be reproduced to a few percent accuracy with a careful choice of Gaussian wave function, as shown in Ref. [21].

For typical cold atomic gas setups, one has harmonically trapped atoms interacting via short-ranged interactions. In the idealized limit of zero-range interactions, the two-body problem is exactly solvable, as demonstrated by Busch *et al.* [16]. In Ref. [15], the exact solution was used to fit the oscillator parameters that provide the input for the harmonic approximation. In the strongly bound limit where a deep two-body bound state occurs, this choice of parameters leads to the same scaling of the energy with particle number that is observed in variational approaches [40,41]. Also, when the interactions have a diverging two-body scattering length (the unitarity limit), the two-body wave function becomes similar to the noninteracting wave function in the trap [16] and we therefore expect the harmonic approximation to be very good. These features are clearly seen in the one-dimensional case as discussed in Ref. [42]. As discussed in Ref. [16], the one- and three-dimensional cases are very similar. The scalings away from these limiting cases are similar, but not identical to other approaches. In general, we expect the harmonic approximation to give good qualitative results for strong interactions, but do not expect perfect quantitative agreement with variation or numerics. On the quantitative side, we note that for one-dimensional systems, the three-body energy can be reproduced to within 10% in the strongly bound limit [42]. We thus estimate similar accuracy on the third virial coefficient. At this point we leave the question of how to adjust the two-body parameters of the Hamiltonian and proceed with a general discussion for arbitrary parameters.

The solution to Eq. (13) is found by a coordinate transformation that splits the Hamiltonian into N independent harmonic oscillators with new coordinates and frequencies related to the normal modes of the N-body system. For N identical particles two new normal mode frequencies are produced, that is, the external trap frequency ω_0 corresponding to the center of mass motion and the $N-1$ times degenerate frequency ω_r given by

$$\omega_r^2 = N\omega_{\rm in}^2/2 + \omega_0^2. \tag{14}$$

The degenerate frequencies correspond to different types of intrinsic (relative) motion, which for two particles is simply oscillations in the relative coordinate, but in the general case corresponds to different normal modes of the system. The N-body energy spectrum is

$$E_j = E_{\text{c.m.}} + E_{\text{rel}} + V_S, \quad V_S = \frac{D}{2}N(N-1)V_{sx}, \quad (15)$$

$$E_{\text{c.m.}} = \hbar\omega_0\left(n_0(j) + \frac{D}{2}\right), \quad n_0(j) = \sum_{i=1}^{D} n_{0,i}(j), \quad (16)$$

$$E_{\text{rel}} = \hbar\omega_r\left(n_r(j) + \frac{D}{2}(N-1)\right) + V_S, \quad (17)$$

$$n_r(j) = \sum_{i=1}^{D}\sum_{k=1}^{N-1} n_{k,i}(j) = \sum_{i=1}^{D} n_{r,i}(j), \quad (18)$$

where j is the index of the N-body states. Here $n_{0,i}$ is the number of excitation quanta in the center-of-mass degree of freedom in the ith direction, while $n_{k,i}$ is the number of quanta in the kth of the $N-1$ degenerate ω_r modes in the ith direction. The energy state j is thus given by specifying the number of excitation quanta in each normal mode for all dimensions. Here we have divided into center of mass and relative contributions since in the equal mass case studied here these can be separated completely.

C. Lowest virial coefficients

The partition function for one particle Q_1 is the trivial problem of one particle in an external harmonic trap of D dimension. Since it has no other particles to interact with, the spectrum arises only from center of mass motion for one particle. The partition function is in this case found from Eqs. (8) and (16) to be

$$Q_1 = \left(\frac{\exp(-\Theta_0/2T)}{1-\exp(-\Theta_0/T)}\right)^D = \frac{1}{2^D}\sinh^{-D}\left(\frac{\Theta_0}{2T}\right), \quad (19)$$

where $\Theta_0 = \hbar\omega_0/k_B$.

The partition function for two particles Q_2 is found from Eqs. (8) and (15)–(17) and can be factorized into center of mass and relative contributions. The center of mass piece is completely symmetric in all the coordinates, so it plays no role in determining the overall symmetry of the system. It is just a geometric series in D dimensions and in fact equal to Q_1 since the frequency is that of the external trap.

The relative motion corresponds to the difference between the two individual coordinates. For fermions this motion then must provide the antisymmetry of the wave function corresponding to an odd number of relative oscillator quanta $n_r(j)$ in Eq. (17). The energies are completely specified by the quanta and the related degeneracy is easily counted for the relative motion of two particles. To obtain an analytical closed solution, it is convenient to consider the individual Cartesian quanta. In two dimensions (2D), one merely needs to keep either quanta $n_{r,x}$ or $n_{r,y}$ odd in the x or y direction. In 3D, there are two possibilities, in that all three quanta are odd or two are even and one is odd. With these restrictions the summation in Eq. (8) leads for $D = 2$ to

$$Q_2 = Q_1\left(\frac{\exp(-\Theta_r/T)}{1-\exp(-2\Theta_r/T)}\right)^2\exp(-\Theta_S/T), \quad (20)$$

where $\Theta_S = V_S/k_B$ and $\Theta_r = \hbar\omega_r/k_B$. For $D = 3$, we find instead

$$Q_2 = Q_1\exp(-\Theta_S/T) \times \frac{3\exp(-5\Theta_r/2T) + \exp(-9\Theta_r/2T)}{[1-\exp(-2\Theta_r/T)]^3}. \quad (21)$$

The next terms involve the partition function Q_3 for the three-body system. A completely closed form solution for the partition function is not found and we keep the expression as an energy sum over three-body states. The center of mass summation is again performed analytically and Eqs. (15) and (17) lead to the other factors amounting in total to

$$Q_3 = Q_1\exp(-\Theta_S/T)\sum_{l=0}^{\infty} g_l\exp[-(l+D)\Theta_r/T], \quad (22)$$

where the summation over all states is reduced to run over all integers. The difficulty is then only to know the corresponding degeneracy g_l. This number of states of a given excitation energy is found by the method described in Ref. [28]. The expression in Eq. (22) is formally the same in two and three dimensions, but the degeneracy factors differ substantially. The infinite sum must in practice be truncated at some level of excitation. Ideally this is after convergence is reached. However, this depends strongly on the value of the temperature and we therefore first must decide how large the T values we need to investigate.

The differences between interacting and noninteracting virial coefficients are found from Eqs. (10) and (11). The noninteracting partition functions are structurally the same as the interacting ones, only with Θ_r replaced by Θ_0 and $\Theta_S = 0$. Using the expressions in Eqs. (20), (21), and (22), we can therefore easily find Δb_2 and Δb_3. For Δb_2 in two dimensions we explicitly get

$$\Delta b_2 = \exp(-\Theta_S/T)\left(\frac{\exp(-\Theta_r/T)}{1-\exp(-2\Theta_r/T)}\right)^2 - \left(\frac{\exp(-\Theta_0/T)}{1-\exp(-2\Theta_0/T)}\right)^2 \quad (23)$$

and a slightly more complicated expression for three dimensions from Eq. (21). In the same way we can of course rewrite Δb_3 in terms of the expression for Q_3 in Eq. (22), but due to the lack of closed form it does not provide any further information.

Notice that the low-temperature limit of the virial coefficients above is determined by the value of the shift Θ_S. From Eq. (23) we see that Δb_2 will vanish for $T \to 0$ whenever we have $\Theta_S + 2\Theta_r > 0$ and similarly for the higher virial coefficients. In the following we will discuss mostly the case $\Theta_S = 0$, i.e., no shift at all, since this is the relevant case for thermodynamics. For generality, we comment briefly on the influence of the shift for all temperatures in Sec. III.

D. High-temperature limits

At high temperature, the interacting system should approach a noninteracting system as the kinetic energy dominates the potential. This does not imply that all Δb_i must vanish at large T, since deviations in the low-energy spectrum between interacting and noninteracting systems easily produce different

large-temperature contributions. This can be seen by dividing the sum over states in the partition functions in low- and high-energy parts. Even if we assume that the high-energy interacting and noninteracting spectra become equal and would thus not contribute to Δb_i, the low-energy parts remains different and this yields a contribution to the virial coefficient for all temperatures. However, such a difference must remain finite since it arises from a finite energy interval.

As stated before, the virial expansion does not work for potentials that do not vanish at a fast enough rate, so one would think that the harmonic potential, which does not vanish at all, would cause problems. Indeed, if we use the derived expressions all our Δb_i diverge with increasing temperature. The origin of this problem is simply that the energy spectrum is obtained for the N-body solution of a temperature-independent Hamiltonian adjusted to reproduce ground-state properties. This does not account for the influence of temperature on the effective interactions and in turn on the energy spectrum. This may also be expressed in terms of an excitation energy dependence of the effective interaction as seen, for example, in the variation of the mean free path. Since excitation energy on average can be related to temperature, these formulations are equivalent.

To pinpoint the problem and subsequently resolve it we start with Δb_2. In the limit of high temperature, Eq. (23) can be expanded to leading orders in T to give

$$\Delta b_2(T\to\infty) = T^2\left(\frac{1}{4\Theta_r^2}-\frac{1}{4\Theta_0^2}\right) - T\frac{\Theta_S}{4\Theta_r^2}. \quad (24)$$

Equivalently, we find for three dimensions that

$$\Delta b_2(T\to\infty) = T^3\left(\frac{1}{2\Theta_r^3}-\frac{1}{2\Theta_0^3}\right) - T^2\frac{\Theta_S}{2\Theta_r^3} + \frac{T}{4}\left(\frac{\Theta_S^2}{\Theta_r^3}+\frac{15}{\Theta_r}-\frac{15}{\Theta_0}\right). \quad (25)$$

Obviously Δb_2 diverges as T to the power of the dimension D, unless of course interacting and noninteracting frequencies are precisely equal. The following orders are independent of T or vanishing with increasing T.

The unphysical divergence is here clearly seen to originate from the difference between the energy spacing found by a fit to ground-state properties and the spacing for a noninteracting system. The proper thermodynamics requires a correct spectrum for all energies or temperatures.

In order for Δb_2 to be finite at large temperatures, ω_r must approach ω_0. From Eq. (14) this seems most reasonably achieved by a vanishing interaction frequency $\omega_{\rm in}$. Furthermore, Eqs. (24) and (25) imply that the energy shift adjusted to fit the ground-state energy also must vanish in the large-temperature limit. To get finite Δb_2 we introduce cutoff functions $F(T)$ and $G(T)$ into $\omega_{\rm in}$ and V_S:

$$\omega_r^2 = \frac{N}{2}F(T)\omega_{\rm in}^2+\omega_0^2, \quad V_S\to V_S G(T). \quad (26)$$

Without further constraints, there is a great deal of freedom in the form of $F(T)$ and $G(T)$, but they must satisfy the conditions of approaching zero respectively as $1/T^D$ and $1/T^{D-1}$ at high temperatures. The simplest such functions

$$F(T) = \left(\frac{T_0}{T+T_0}\right)^D, \quad G(T) = \left(\frac{T_0}{T+T_0}\right)^{(D-1)}, \quad (27)$$

where T_0 is a cutoff parameter that indicates at what temperature the spectrum continuously should shift to the noninteracting spectrum. These functions regularize the high-temperature behavior and now Δb_2 approaches a constant at high temperatures. The limits in the different dimensions can be found from Eqs. (24) and (25) by use of Eqs. (26) and (27), that is,

$$\Delta b_2(T\to\infty) = -\frac{N}{8}\frac{\omega_{\rm in}^2}{\omega_0^2}\frac{(k_BT_0)^2}{(\hbar\omega_0)^2} - \frac{V_S k_B T_0}{4(\hbar\omega_0)^2} \quad (28)$$

for two dimensions, and for three dimensions we get

$$\Delta b_2(T\to\infty) = -\frac{3N}{8}\frac{\omega_{\rm in}^2}{\omega_0^2}\frac{(k_BT_0)^3}{(\hbar\omega_0)^3} - \frac{V_S(k_BT_0)^2}{2(\hbar\omega_0)^3}, \quad (29)$$

where $N=2$ for this second virial coefficient. The high-temperature limit is then determined by the interaction frequency, the ground-state energy shift, and the cutoff temperature. The two terms have opposite sign since V_S is negative and initially introduced to balance the zero-point energy of the oscillator such that large $\omega_{\rm in}$ is correlated with a large negative V_S.

Once Δb_2 is regularized we turn to Δb_3, which is more complex, as seen in Eq. (11). It consists of two terms, the difference between interacting and noninteracting partition functions for three particles and $\Delta Q_2 = Q_1\Delta b_2$. This latter term contains the already regularized factor Δb_2, but Q_1 in Eq. (19) also diverges as $\to T^D/\Theta_0^D$ at high temperature. Therefore Δb_3 can only remain finite in the limit when the difference $(Q_3 - Q_3^{(1)})/Q_1$ diverges precisely as Q_1.

However, this is not even sufficient because the T^D divergence from Q_1 leads to divergence of the terms in Δb_2 vanishing as $1/T$ in two dimensions and as $1/T$ and $1/T^2$ in three dimensions. These terms all must be canceled by corresponding diverging terms in $(Q_3 - Q_3^{(1)})/Q_1$. These conditions seem impossible to meet, but nevertheless this miracle seems to occur. We find that Δb_3 also is regularized with precisely the same cutoff function as used for Δb_2 and this occurs in both two and three dimensions. Problems with divergences in Δb_3 have been reported by other authors [43]. They resolved it by separating the system into a $2+1$ subsystem in which the divergence was then removed. While we do not need to do this to obtain a finite Δb_3, the underlying deep reason for this is still unclear to us.

The form of the cutoff in Eq. (26) can be changed in many ways. The transition can set in at different temperatures and be more or less fast. We have chosen to use only one parameter T_0, but we tested with another functional form

$$F(T) = [1-\exp(-T_0/T)]^D, \quad (30)$$

which has the same high-temperature behavior. Both Δb_2 and Δb_3 are again regularized in the high-temperature limit. The values of Δb_2 and Δb_3 are both larger in magnitude at all temperatures simply because this cutoff function is larger for all T.

Instead of the temperature cutoff in Eq. (26), we could choose a cutoff in excitation energy. This might at first appeal as being more physically reasonable since this directly amounts to changing the N-body spectrum at high excitation energy to the noninteracting N-body spectrum. However, this conclusion is rather shaky. Completely different configurations specified by sets of quantum numbers can give precisely the same energy. This is easily seen in a single-particle picture by comparing states of the same total energy arising from a few particles at very high-lying levels and all others in the lowest possible levels with the opposite where all particles are in levels of intermediate energy.

Thus a given excitation energy already corresponds to an average over many configurations very similar to the configurations occupied for a given temperature. In any case, we investigated a cutoff in excitation energy instead of temperature, that is, expressions of simplicity similar to those in Eq. (27):

$$F(E) = \left(\frac{E_0}{E+E_0}\right)^D, \quad G(E) = \left(\frac{E_0}{E+E_0}\right)^{(D-1)}, \quad (31)$$

where E is the excitation energy. This function is inserted in Eq. (26) in the place of $F(T)$ and when the partition function is being calculated as the sum over states, the step in energy taken between states is now dependent on the position in the spectrum. The mean field spacing is reached for energies higher than E_0. Implementing this cutoff successfully regularizes Δb_2, but to remove the divergence for Δb_3 it is necessary to use a constant E_0 different from that of Δb_2. No obvious relation is found and generalizations to higher Δb_i seem to be at least very impractical.

III. NUMERICAL RESULTS

The virial coefficients can now be calculated numerically. In the model they are completely determined from trap frequency ω_0, interaction frequency $\omega_{\rm in}$, shift energy V_S, and cutoff function and related parameters T_0. We use the trap frequency as the energy unit, which implies that results for any other value of ω_0 can be obtained by scaling all energies $\hbar\omega_{\rm in}$, $k_B T_0$, and V_S by $\hbar\omega_0$. The energy shift V_S is introduced to adjust to the correct energy and has no effect on eigenvalues and corresponding wave functions. It is strongly dependent on which model is approximated. We shall therefore first investigate the general dependencies on $\omega_{\rm in}$ and T_0, which in turn can be related to specific models. Afterwards we shall separately investigate the dependence on the shift.

A. Virial coefficients

The cutoff parameter is essential for the behavior of the expansion coefficients. The size of an appropriate value can be estimated by inspection of the effect it is designed to simulate. The first excited state appears at an excitation energy of $\hbar\omega_r$, which is a single-quasiparticle excitation. Therefore $\hbar\omega_r$ represents a shell gap to be overcome by thermal excitations. This gap is known to wash out at a critical temperature T, given by $k_B T 2\pi^2 \approx \hbar\omega_r$ (see Refs. [44,45]). This surprisingly large factor $2\pi^2 \approx 19.7$ suggests a rather small relative value of T_0 proportional to ω_r, that is, $k_B T_0 \approx \hbar\omega_r/2\pi^2$.

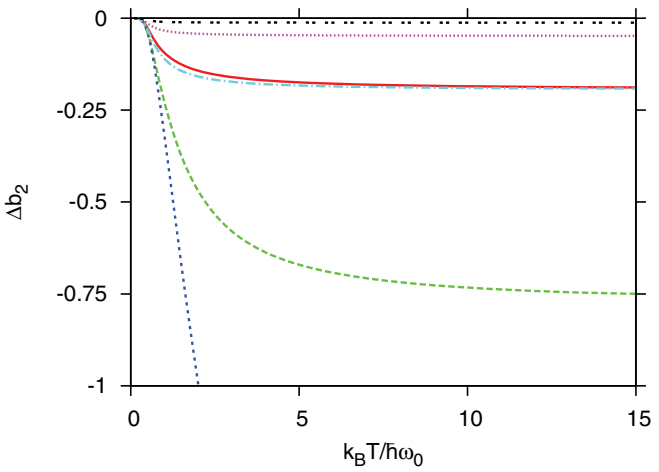

FIG. 1. (Color online) Virial coefficient Δb_2 in 2D as a function of temperature with a model space of 160 oscillator shells and zero energy shift. The cutoff used was the function in Eq. (27). The values of T_0 and $\omega_{\rm in}$ (in units of ω_0) from bottom to top are $(T_0,\omega_{\rm in}) = (0.51,5.0)$, $(0.25,5.0)$, $(0.13,5.0)$, $(0.25,2.5)$, $(0.13,5.0)$, and $(0.062,2.5)$. The T_0 values are $\omega_{\rm in}/2\pi^2$ and twice and half that value.

To illustrate the dependence we show Δb_2 in Fig. 1 as a function of T for different interactions and cutoff values. We see the general behavior of a second-order increase from zero at $T = 0$ and the smooth curvature before bending over to reach the saturation value. The expansion coefficient is a rather strongly increasing function of both interaction frequency and cutoff parameter. The functional form of the cutoff function in Eq. (27) implies that the saturation value and saturation temperature both depend rather strongly on T_0.

The overall behavior must be understood in the model even at uninterestingly high temperatures. We continue to show Δb_3 in Fig. 2 for two dimensions for the same set of parameters as in Fig. 1, with qualitatively the same behavior, except for the overall opposite sign. However, the temperature dependence is faster and the saturation values are larger, as seen for the small interaction frequency with the small T_0. For higher values

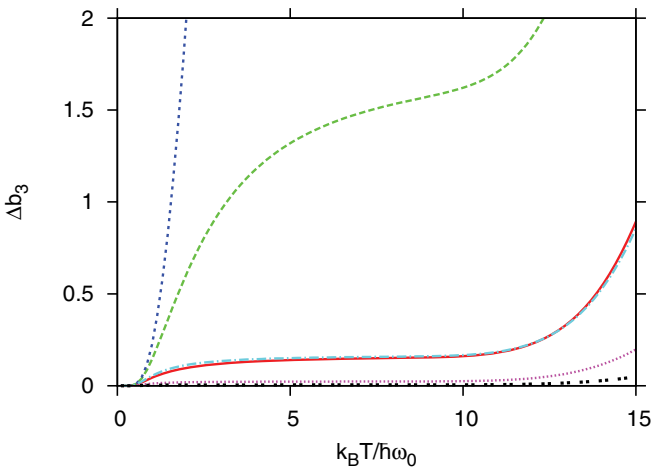

FIG. 2. (Color online) Same as in Fig. 1 for Δb_3 in 2D. The parameters are also the same, but must be read from top to bottom.

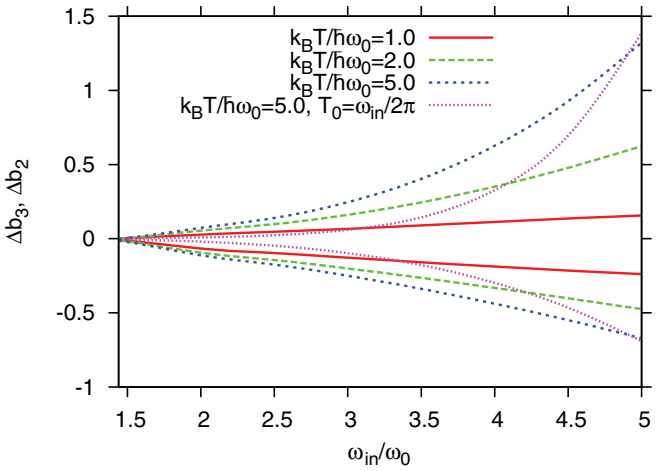

FIG. 3. (Color online) Virial coefficients $\Delta b_2 < 0$ and $\Delta b_3 > 0$ as a function of interaction frequency ω_{in} for three different temperatures. Notice that from Eq. (14) we always have $\omega_{\text{in}} > \sqrt{2}\omega_0$. On this plot $k_B T_0/\hbar\omega_0 = 0.25$ for all curves except the dotted line, which has $k_B T/\hbar\omega = 5.0$ and $k_B T_0 = \hbar\omega_{\text{in}}/2\pi^2$ (adjusted at the end point on the horizontal axis).

we observe a tendency to form a flat region, which quickly becomes an increasing function.

At low temperature, the coefficients vanish since both the interacting and noninteracting partition functions go to unity at low temperature (in the absence of any energy shift). This might seem odd since our Δb_i's are the difference between a noninteracting and an interacting system, which should increase at low temperatures when the interactions are more significant compared to the kinetic energy. Since both of the partition functions are small at low temperature, the only signature we see of this is that the relative difference of the partition functions, for example, $(Q_2 - Q_2^{(i)})/Q_2^{(i)}$, does increase.

The effect of the interaction frequency is plainly to increase the virial coefficient, which could be seen in Figs. 1 and 2. A more precise dependence on interaction frequency can be seen in Fig. 3. The coefficients vanish for small ω_{in}, as then there is no difference between the noninteracting and interacting systems, but then increase rapidly, especially after $\omega_{\text{in}} > \omega_0$. The increase is more dramatic at higher temperatures, which are closer to the saturation value. It does appear, however, that for any temperature the behavior of the coefficients is faster than linear.

B. Hilbert space and cutoff function

The apparent lack of saturation for Δb_3 at high temperatures is a very unsatisfactory feature. Fortunately, it seems to be an effect of the model space truncation at high excitation energies in the calculation of the partition function. This happens because of the subtle nature of the cancellation that removes the divergence and leads to saturation. The piece Q_1 in ΔQ_2 in Eq. (11) contains all states to infinitely high excitation energies since it is calculated analytically. This piece eventually overwhelms the ΔQ_3 term in Eq. (11), which is calculated numerically and consequently arises from a truncated energy spectrum.

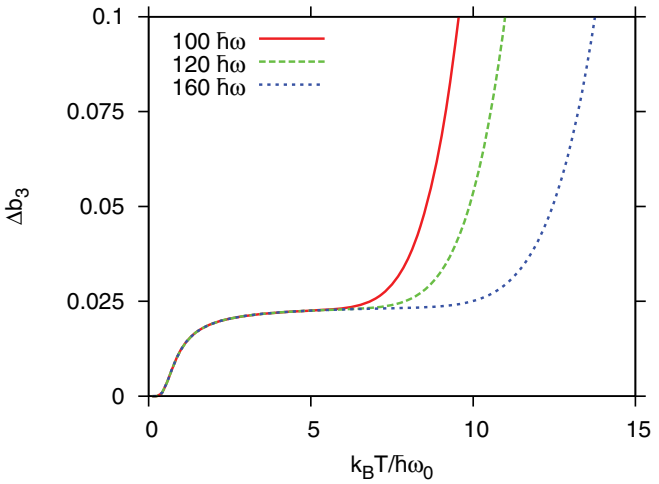

FIG. 4. (Color online) Virial coefficient Δb_3 in 2D as a function of temperature for three different model space sizes. The cutoff function is that given in Eq. (27). The other parameters are $k_B T_0 = 0.25\hbar\omega_0$ and $\omega_{\text{in}} = 2.5\omega_0$.

We demonstrate this in Fig. 4, where we show Δb_3 for three different model space sizes. The higher the energies we include in the numerical calculation, the larger the region of the flat saturation interval and the larger the temperatures before the divergence sets in. This is very reassuring, allowing us to ignore the unphysical region of all temperatures above the flat region.

One uncertainty in the method to recover the high-energy noninteraction limit is the function describing the disappearance of shell effects. In Fig. 5 we illustrate this dependence of the virial coefficients by results from use of different cutoff functions, that is, the rational expression [Eq. (27)] and the exponential function [Eq. (30)]. The virial coefficients using the exponential cutoff are larger for all temperatures before finally merging into the same high-temperature limit. This is due to the larger cutoff function at all temperatures, which

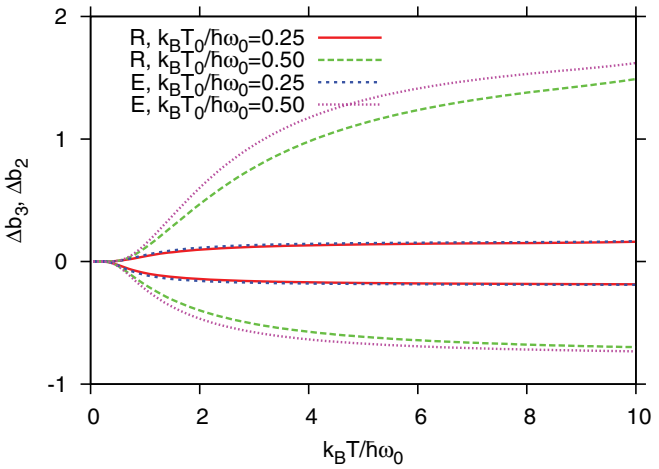

FIG. 5. (Color online) Virial coeffecients in 2D as a function of temperature for different cutoff functions. The rational function cutoffs [Eq. (27)] are labeled with an R and the exponential cutoff [Eq. (30)] is labeled with an E. Here $\omega_{\text{in}} = 2.5\omega_0$ was used for all the curves.

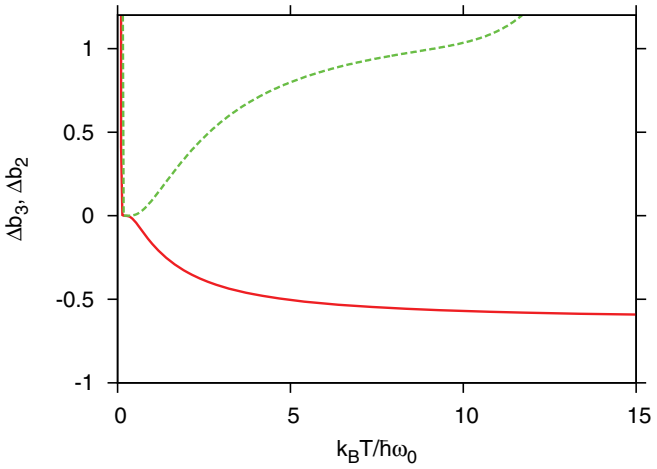

FIG. 6. (Color online) Virial coefficients Δb_2 (bottom solid line) and Δb_3 (top dashed line) in 2D as a function of temperature examining the effect of the energy shift. The coefficients behave similarly to what was shown previously, except at very low temperature. For this plot $\omega_{\rm in} = 2.0\omega_0$ with $V_s = -5.81\hbar\omega_0$ and $k_B T_0 = 0.5\hbar\omega$.

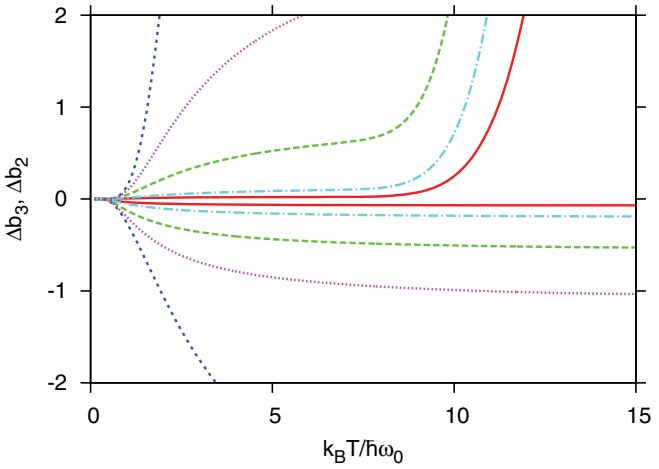

FIG. 7. (Color online) Virial coefficients in three dimensions, $\Delta b_2 < 0$ (lines on the bottom half of the graph) and $\Delta b_3 > 0$ (lines on the top half of the graph), as functions of temperature. The cutoff temperature T_0 and $\omega_{\rm in}$ are varied among the different curves. On the Δb_2 side (below zero), from bottom to top, $(k_B T_0/\hbar\omega_0, \omega_{\rm in}/\omega_0) = (1.00, 2.5)$, $(0.50, 3.5)$, $(0.50, 2.5)$, $(0.50, 1.5)$, and $(0.25, 2.5)$. For Δb_3 (above zero), the lines have the parameters just listed, but in inverse order. For this plot there is no energy shift $V_S = 0$ and a model space of 160 shells is used.

leaves the reduction to take place somewhat faster at larger temperatures, although the same final saturation is reached for T much larger than T_0.

C. Effect of the energy shift

The energy shift in the Hamiltonian has a different effect on the virial coefficient. We illustrate by the examples in Fig. 6. The high-temperature limit remains finite by construction, as shown explicitly in energies [Eq. (28)] for one case. Otherwise the behavior at high T is very similar to that of zero shift, where convergence is essential or at least a flat region at high T is necessary. The energies enter in the partition function in the exponent. Contributions disappear from energies much higher than the temperature.

However, at very low temperatures the same contribution from the shift can produce unphysical results. This is seen at very low T in Fig. 6, where a narrow and large peak is present in both virial coefficients. The numerical reason is obvious since the negative shift divided by a small temperature value produces a very large value. This occurs for temperatures much smaller than ω_0 and long before the statistical treatment is meaningful.

The negative shift is not necessarily sufficient for a divergence at low temperatures. The shift energy must completely eliminate the zero-point energy and thus for polarized fermions $V_S < -DN\hbar\omega_r$. The parameters in Fig. 6 provide a shift large enough in magnitude to give a spike towards large positive values at very low temperatures. This changes the sign of Δb_2, as the term containing the shift (small T) eventually becomes larger than the noninteracting term in Eq. (23).

For Δb_3, the singularity at zero temperature comes at a slightly higher temperature since the shift energy is three times larger than for two particles. Again this occurs for temperatures lower than those allowing a statistical treatment.

D. Three dimensions

We have so far shown results for only two dimensions. The method is, however, applicable in three dimensions, where the coefficients look qualitatively similar to those in two dimensions (see Fig. 7). We notice the increase from zero at $T = 0$, then a decreasing derivative resulting in saturation or in a tendency towards saturation, and finally the divergence at high temperature for Δb_3 due to mismatch between the numerical Q_3 and the analytical Q_1. The results are more sensitive to the cutoff parameter because powers that enter in two dimensions are higher than in three dimensions, as seen, for example, by comparing Eqs. (28) and (29). Indeed, if one uses $T_0 = \omega_{\rm in}/2\pi^2$, then the magnitude of the coefficients is quite small, of order 10^{-2}. Also, the truncation effect in Δb_3 is more sensitive to the cutoff parameter and can begin at comparatively low temperatures when compared to 2D (see Fig. 2).

The virial expansion is most efficient when the size of the coefficients decrease with the order. Therefore, a requirement of $\Delta b_3 \leqslant \Delta b_2$ leads to a condition on the maximum size of T_0. This demand is more restrictive for three dimensions than for two dimensions.

IV. SUMMARY AND OUTLOOK

We have discussed the virial expansion technique and a quantum mechanical formulation was sketched from an analogous classical expansion. We applied the formulated method to a harmonic approximation to the N-body problem for identical fermions. A key step in this approach was the adjustment of the harmonic one- and two-body parameters to pertinent properties of the corresponding two-body problem that holds information about the exact interaction that is approximated by a harmonic form. Once these were obtained, the resulting

N-body Schrödinger equation could be solved exactly and the spectrum could be used to compute the partition function. The second- and third-order virial expansion coefficients were obtained by direct calculation of the two- and three-body partition functions. Here we were interested in the details of the formal development of a virial expansion and we therefore varied the parameters of the harmonic interaction terms freely to study the behavior. The mapping to realistic two-body properties was straightforward.

The virial expansion could be reformulated in terms of deviations between noninteracting and interacting systems. Importantly, the virial coefficients have an unphysical divergence for large temperatures. It arises in the formulation because the increasing temperature populates higher and higher excited states. Their average properties can be very far from the ground-state properties and eventually the results should resemble those of the noninteracting system where the kinetic energy is decisive. This was achieved by modifying the energy spectrum by a function of temperature smoothly connecting the low-temperature ground-state dominated and high-temperature noninteracting spectra.

To achieve the goal of removing the divergence, the modification function must reduce the initial interaction frequency to zero by a high-temperature behavior where the power of the temperature is equal to the spatial dimension of the system. The divergence was removed from the second-order expansion coefficient and it turned out that the same modification function removed the divergence from the third-order term. This result is highly nontrivial since the third-order divergence is of a very different origin from that of second order. This was emphasized by an attempt to use an energy- (in contrast to temperature-) dependent modification function, which removed the second-order divergence but required an additional adjustment to remove the third-order divergence. The temperature modification is then the more promising approach for applications where higher orders have to be calculated.

We found that the critical temperature value describing where the adjustment of the spectrum should take place and the rate of the modification should be about $2\pi^2$ smaller than the two-body interaction frequency. This is analogous to the smearing of shell effects by temperature in an N-body finite system described by its single-particle spectrum. This function is exponential and the rate is precisely the single-particle frequency divided by $2\pi^2$. In our case the modification function was chosen to have a rate of change of the N-body energy spectrum that is a rational function of temperature to a power that depends on dimension. However, the modification took place on the energies appearing in the exponent of the partition function. The precise shape of the temperature modification function is not essential for the overall properties unless one considers extreme cases. A sensible choice of modification function that regularizes the divergence will thus yield a formalism that can be adjusted to low-energy properties and make further predictions for the many-body problem.

While we have focused on two- and three-dimensional systems in the current presentation, a good testing ground for the formalism discussed would be some of the exactly solvable models that are known in one-dimensional systems [46]. A good example is the N-boson problem with zero-range interactions studied by Lieb, Linniger, and MacGuire [47] for which the harmonic approximation can be applied [42] or to dipolar molecules in one-dimensional setups where N-body clusterized bound states can easily form [48]. In the strong-coupling domain these should be well described within a harmonic approximation approach.

In summary, we have demonstrated that the harmonic approximation employed at the Hamiltonian level gives a divergent set of virial expansion coefficients that must be regularized at high temperature. This can be done by a careful choice of temperature-dependent spectral modification that will render the virial coefficients finite at all temperatures. The ease of solving the harmonic N-body problem and subsequently calculating the virial coefficients makes this an attractive approach to compute many-body properties.

[1] M. Thiesen, Ann. Phys. (Leipzig) **24**, 467 (1885).

[2] H. K. Onnes, Commun. Phys. Lab. Univ. Leiden **71**, 3 (1901).

[3] H. D. Ursell, Math. Proc. Cambridge Philos. Soc. **23**, 685 (1927).

[4] T. L. Hill, *Statistical Mechanics* (McGraw-Hill, New York, 1956).

[5] E. Beth and G. E. Uhlenbeck, Physica **4**, 915 (1937); B. Kahn and G. E. Uhlenbeck, *ibid.* **5**, 399 (1938).

[6] K. Huang, *Statistical Mechanics*, 2nd ed. (Wiley, New York, 1987).

[7] R. Dashen, S.-K. Ma, and H. J. Bernstein, Phys. Rev. **187**, 345 (1969).

[8] S. K. Adhikari and R. D. Amado, Phys. Rev. Lett. **27**, 485 (1971).

[9] P.-T. How and A. LeClair, Nucl. Phys. B **824**, 415 (2010); J. Stat. Mech. (2010) P0302; (2010) P07001.

[10] A. LeClair, E. Marcelino, A. Nicolai, and I. Roditi, Phys. Rev. A **86**, 023603 (2012).

[11] F. Brosens, J. T. Devreese, and L. F. Lemmens, Phys. Rev. E **55**, 227 (1997); **55**, 6795 (1997); **57**, 3871 (1998); **58**, 1634 (1998).

[12] M. A. Zaluska-Kotur, M. Gajda, A. Orlowski, and J. Mostowski, Phys. Rev. A **61**, 033613 (2000); J. Yan, J. Stat. Phys. **113**, 623 (2003); M. Gajda, Phys. Rev. A **73**, 023603 (2006).

[13] F. Brosens, J. T. Devreese, and L. F. Lemmens, Phys. Rev. A **55**, 2453 (1997); J. Tempere, F. Brosens, L. F. Lemmens, and J. T. Devreese, *ibid.* **58**, 3180 (1998); **61**, 043605 (2000); L. F. Lemmens, F. Brosens, and J. T. Devreese, *ibid.* **59**, 3112 (1999); S. Foulon, F. Brosens, J. T. Devreese, and L. F. Lemmens, Phys. Rev. E **59**, 3911 (1999).

[14] J. Tempere, F. Brosens, L. F. Lemmens, and J. T. Devreese, Phys. Rev. A **61**, 043605 (2000).

[15] J. R. Armstrong, N. T. Zinner, D. V. Fedorov, and A. S. Jensen, J. Phys. B **44**, 055303 (2011).

[16] T. Busch, B. G. Englert, K. Rzażewski, and M. Wilkens, Found. Phys. **28**, 548 (1998).

[17] T. Stöferle, H. Moritz, K. Günter, M. Köhl, and T. Esslinger, Phys. Rev. Lett. **96**, 030401 (2006); T. Volz, N. Syassen, D. M. Bauer, E. Hansis, S. Dürr, and G. Rempe, Nat. Phys. **2**, 692 (2006); G. Thalhammer, K. Winkler, F. Lang, S. Schmid, R. Grimm, and J. H. Denschlag, Phys. Rev. Lett. **96**, 050402 (2006); C. Ospelkaus, S. Ospelkaus, L. Humbert, P. Ernst, K. Sengstock, and K. Bongs, *ibid.* **97**, 120402 (2006).

[18] W. C. Haxton and T. Luu, Phys. Rev. Lett. **89**, 182503 (2002); I. Stetcu, B. R. Barrett, and U. van Kolck, Phys. Lett. B **653**, 358 (2007); I. Stetcu, B. R. Barrett, U. van Kolck, and J. P. Vary, Phys. Rev. A **76**, 063613 (2007); Y. Alhassid, G. F. Bertsch, and L. Fang, Phys. Rev. Lett. **100**, 230401 (2008); N. T. Zinner, K. Mølmer, C. Özen, D. J. Dean, and K. Langanke, Phys. Rev. A **80**, 013613 (2009); I. Stetcu, J. Rotureau, B. R. Barrett, and U. van Kolck, Ann. Phys. (N.Y.) **325**, 1644 (2010); T. Luu, M. J. Savage, A. Schwenk, and J. P. Vary, Phys. Rev. C **82**, 034003 (2010); J. Rotureau, I. Stetcu, B. R. Barrett, M. C. Birse, and U. van Kolck, Phys. Rev. A **82**, 032711 (2010).

[19] J. R. Armstrong, N. T. Zinner, D. V. Fedorov, and A. S. Jensen, Europhys. Lett. **91**, 16001 (2010); Few-Body Syst., arXiv:1112.6141 (to be published); D. V. Fedorov, J. R. Armstrong, N. T. Zinner, and A. S. Jensen, Few-Body Syst. **50**, 395 (2011).

[20] J. R. Armstrong, N. T. Zinner, D. V. Fedorov, and A. S. Jensen, Eur. Phys. J. D **66**, 85 (2012); A. G. Volosniev, J. R. Armstrong, D. V. Fedorov, A. S. Jensen, and N. T. Zinner, Few-Body Syst., arXiv:1112.2541 (to be published).

[21] N. T. Zinner, J. R. Armstrong, A. G. Volosniev, D. V. Fedorov, and A. S. Jensen, Few-Body Syst., arXiv:1105.6264 (to be published).

[22] D.-W. Wang, M. D. Lukin, and E. Demler, Phys. Rev. Lett. **97**, 180413 (2006).

[23] A. Pikovski, M. Klawunn, G. V. Shlyapnikov, and L. Santos, Phys. Rev. Lett. **105**, 215302 (2010); N. T. Zinner, B. Wunsch, D. Pekker, and D.-W. Wang, Phys. Rev. A **85**, 013603 (2012).

[24] S.-M. Shih and D.-W. Wang, Phys. Rev. A **79**, 065603 (2009).

[25] M. Klawunn, A. Pikovski, and L. Santos, Phys. Rev. A **82**, 044701 (2010).

[26] M. A. Baranov, A. Micheli, S. Ronen, and P. Zoller, Phys. Rev. A **83**, 043602 (2011).

[27] A. G. Volosniev, D. V. Fedorov, A. S. Jensen, and N. T. Zinner, Phys. Rev. Lett. **106**, 250401 (2011); Phys. Rev. A **85**, 023609 (2012); A. G. Volosniev, N. T. Zinner, D. V. Fedorov, A. S. Jensen, and B. Wunsch, J. Phys. B **44**, 125301 (2011).

[28] J. R. Armstrong, N. T. Zinner, D. V. Fedorov, and A. S. Jensen, Phys. Rev. E **85**, 021117 (2012).

[29] L. F. Lemmens, F. Brosens, and J. T. Devreese, Solid State Commun. **109**, 615 (1999).

[30] S. N. Klimin, V. M. Fomin, F. Brosens, and J. T. Devreese, Phys. Rev. B **69**, 235324 (2004).

[31] F. Brosens, S. N. Klimin, and J. T. Devreese, Phys. Rev. B **71**, 214301 (2005).

[32] M. Horikoshi, S. Nakajima, M. Ueda, and T. Makaiyama, Science **327**, 442 (2010); S. Nascimbéne *et al.*, Nature (London) **463**, 1057 (2010); N. Navon, S. Nascimbéne, F. Chevy, and C. Salomon, Science **328**, 729 (2010); C. Cao *et al.*, *ibid.* **331**, 58 (2011); M. J. H. Ku, A. T. Sommer, L. W. Clark, and M. W. Zwierlein, *ibid.* **335**, 563 (2012).

[33] T.-L. Ho and E. J. Mueller, Phys. Rev. Lett. **92**, 160404 (2004); H. Hu, P. D. Drummond, and X.-J. Liu, Nat. Phys. **3**, 469 (2007); X.-J. Liu, H. Hu, and P. D. Drummond, Phys. Rev. Lett. **102**, 160401 (2009); Phys. Rev. A **82**, 023619 (2010); S.-G. Peng, S.-Q. Li, P. D. Drummond, and X.-J. Liu, *ibid.* **83**, 063618 (2011); X. Leyronas, *ibid.* **84**, 053633 (2011); D. B. Kaplan and S. Sun, Phys. Rev. Lett. **107**, 030601 (2011).

[34] J. E. Mayer and M. G. Mayer: *Statistical Mechanics* (Wiley, New York, 1940).

[35] L. E. Reichl, *A Modern Course in Statistical Physics*, 2nd ed. (Wiley, New York, 1998).

[36] H. Hu, X.-J. Liu, and P. D. Drummond, New J. Phys. **12**, 063038 (2010).

[37] Z. Idziaszek and T. Calarco, Phys. Rev. Lett. **96**, 013201 (2006); Z. Idziaszek, Phys. Rev. A **79**, 062701 (2009).

[38] K. Kanjilal and D. Blume, Phys. Rev. A **73**, 060701(R) (2006); N. T. Zinner, J. Phys. A **45**, 205302 (2012).

[39] P. K. Sørensen, D. V. Fedorov, A. S. Jensen, and N. T. Zinner, arXiv:1206.2274.

[40] R. V. E. Lovelace and T. J. Tommila, Phys. Rev. A **35**, 3597 (1987); G. Baym and C. J. Pethick, Phys. Rev. Lett. **76**, 6 (1996).

[41] H. Fu, Y. Wang, and B. Gao, Phys. Rev. A **67**, 053612 (2003); N. T. Zinner and M. Thøgersen, *ibid.* **80**, 023607 (2009); N. T. Zinner, arXiv:0909.1314; M. Thøgersen, N. T. Zinner, and A. S. Jensen, Phys. Rev. A **80**, 043625 (2009).

[42] J. R. Armstrong, N. T. Zinner, D. V. Fedorov, and A. S. Jensen, Physica Scripta, arXiv:1205.0717 (to be published).

[43] X.-J. Liu, H. Hu, and P. D. Drummond, Phys. Rev. B **82**, 054524 (2010).

[44] A. S. Jensen and J. Damgaard, Nucl. Phys. A **203**, 578 (1973).

[45] A. Bohr and B. R. Mottelson, *Nuclear Structure, Vol. 1* (Benjamin, New York, 1969).

[46] B. Sutherland, *Beautiful Models* (World Scientific, Singapore, 2004); R. J. Baxter, *Exactly Solved Models in Statistical Mechanics* (Academic, New York, 1982); V. E. Korepin, *Exactly Solvable Models of Strongly Correlated Electrons* (World Scientific, Singapore, 1994).

[47] E. Lieb and W. Liniger, Phys. Rev. **130**, 1605 (1963); E. Lieb, *ibid.* **130**, 1616 (1963); J. MacGuire, J. Math. Phys. **5**, 622 (1964).

[48] B. Wunsch, N. T. Zinner, I. B. Mekhov, S. J. Huang, D. W. Wang, and E. Demler, Phys. Rev. Lett. **107**, 073201 (2011); M. Dalmonte, P. Zoller, and G. Pupillo, *ibid.* **107**, 163202 (2011); N. T. Zinner, B. Wunsch, I. B. Mekhov, S. J. Huang, D. W. Wang, and E. Demler, Phys. Rev. A **84**, 063606 (2011); M. Knap, E. Berg, M. Ganahl, and E. Demler, Phys. Rev. B **86**, 064501 (2012); M. Bauer and M. M. Parish, Phys. Rev. Lett. **108**, 255302 (2012).